14th International Conference on Applications of Statistics and Probability in Civil Engineering, ICASP14
Dublin, Ireland, July 9-13, 2023

Effects of Climate Changes and Spatial Soil Moisture Variability on the Geomechanical Response of Segmented Buried Pipes

Sidi Mohammed Elachachi
Professor, University of Bordeaux, I2M-GCE, UMR 5295, 33400 Talence, France

Humberto Yáñez-Godoy
Associate Professor, University of Bordeaux, I2M-GCE, UMR 5295, 33400 Talence, France

Zoubir-Mehdi Sbartai
Professor University of Bordeaux, I2M-GCE, UMR 5295, 33400 Talence, France

Ghina Darwich
PhD, University of Bordeaux, I2M-GCE, UMR 5295, 33400 Talence, France

ABSTRACT: Moisture content of soils as well as the geomechanical soil properties are affected by seasonal fluctuations in temperature and rainfall. This phenomenon is even more amplified when climate change issue is considered. In the case of segmented buried pipes, the soil-structure interaction which drive the global behavior of the set of pipes (redistribution of the applied loads, -absolute or differential- settlements, etc.) is also totally impacted by the effects of climate change and therefore leads to pipe failure. In this paper, the focus is on analyzing the effects of the climate change on the response of segmented buried pipes like stormwater or sewer pipes, made of reinforced concrete, by considering three climate scenarios and comparing them to the current climate. To the seasonal variability, we also add the spatial variability of the properties of the soil. A probabilistic and reliability-based analysis is conducted on a simple model which includes the soil-pipe interaction and considers the spatio-seasonal variability of the moisture content of the soil, in order to quantify the effects of the various scenarios on structural, hydraulic and tightness performances of the buried segmented pipes.

Urban water supply, particularly large buried water, stormwater or sewer pipes play core roles in socio-economic development. Among its many current effects, climate change is raising mean temperature and increasing heavy precipitation events (Wols, 2014, Wuebbles et al., 2017). These changes, despite the evolving regulation strategies throughout Europe and France, make these infrastructures more vulnerable. Coverage of all vulnerabilities is beyond the scope of this paper. Rather, for consistency, the focus is on vulnerabilities related to geomechanically behavior of buried segmented pipes to climate variability and long-term change in order to provide answers in the design of climate-resilient infrastructure.

1. CLIMATE CHANGE SCENARIOS

Various climate change scenarios exist depending on the overall emissions pathway and decisions resulting in increased exposure of assets and mal-adaptation (Pachauri, et al., 2014). Three of all the scenarios considered from the Intergovernmental Panel on Climate Change (IPCC) are retained in this study: low emissions (RCP2.6), similar to current (RCP4.5) and high emissions (RCP8.5) pathways (DRIAS, 2021). Figure 1 shows the discrepancies of annual cumulative precipitation for these three scenarios and for three-time horizons of three decades (2021-2050, 2041-2070 and 2071-2100). It should be noted that these climate model projections are subject to significant uncertainty, particularly on a regional or local scale. There is moreover less confidence

in precipitation projections than those for temperature (Shepherd, 2014).

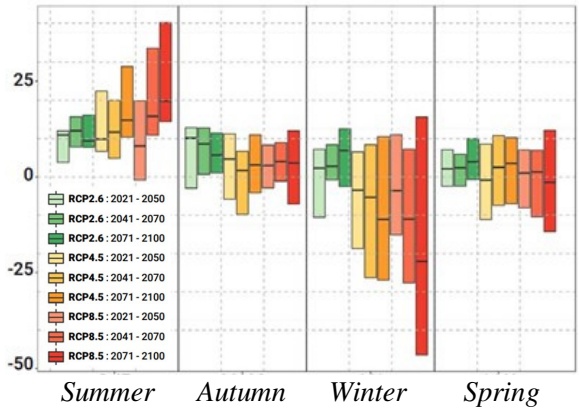

Figure 1: Seasonal evolution of the relative discrepancies of total annual cumulative precipitation accumulation by RCP and time horizon (DRIAS, 2021).

The physical impacts of climate change – such as increasing temperatures, shifting patterns of precipitation, increased intensity or recurrence of extreme weather events are different depending on the climatic areas (Figure 2).

In this study we will focus on the city of Bordeaux in France which is located in an oceanic climatic area.

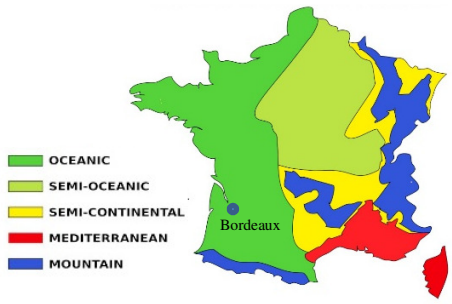

Figure 2: Climatic areas in France.

2. FROM CLIMATE DATA TO SOIL MOISTURE DISTRIBUTION

Links between climate and soil moisture are well known, including the influence of precipitation on point-scale soil moisture distributions and vertical infiltration (Entekhabi et al., 1996).

Soil moisture dynamics at rainfall event scales relies on the studies that use any of the aspects of soil moisture such as changes in volumetric water content, response time, or wetting front velocity (Singh et al., 2021).

The spatial heterogeneity of soil moisture is influenced not only by spatial and temporal (seasonal) precipitation but also by factors such as the lateral redistribution and preferential flow of soil water, the topography, soil properties and being situated in a dense urban area with a lot of runoff or a low-density area with more infiltration in the soil.

Models allowing to transform precipitation into soil water content are quite complex models that depend on many interactions and processes and are intimately linked to the time step used (minute fraction, hourly, weekly or monthly) in the resolution.

For example, with the Richards' model (Rodriguez-Iturbe and Porporato, 2004), the averaged soil moisture balance at a point is expressed by:

$$nz\frac{d\theta}{dt} = P - T - TR \qquad (1)$$

where n is the soil porosity, z the depth, θ the volumetric water content, P, ET, and TR represent, precipitation, evapotranspiration, and horizontal and downward transport of water (runoff and infiltration) respectively. Equation (1) is a stochastic, ordinary differential equation for the state variable θ.

The temporal structure within each rain event is ignored and the marked Poisson process representing precipitation P is physically interpreted at a daily time scale. With these assumptions, the distribution of the times between precipitation events is exponential (Eq. 2) with mean $1/\lambda$ (or an arrival time of λ).

$$f_T(\tau) = \lambda e^{-\lambda\tau} \qquad (2)$$

The marks correspond to the rainfall depth of rainy days, h, modeled as an independent exponentially distributed random variable with mean α (Eq. 3) and which will be one of the inputs of Eq. 1:

$$f_H(h) = \frac{1}{\alpha} e^{-\frac{1}{\alpha}\tau} \quad (3)$$

The values of α and λ are assumed to be season-dependent quantities during the modeling period i.e. precipitation is considered as a "seasonally" stationary stochastic process. Infiltration and runoff are function of the amount of precipitation and soil moisture, being a stochastic and state-dependent component, their magnitude and temporal occurrence are controlled by soil moisture dynamics (Rodriguez-Iturbe and Porporato, 2004). Finally, the soil drying process during no-rain periods, is modeled deterministically (decay of soil moisture depends on the previous history of the soil–drying–wetting process).

The calibration of the various parameters feeding the models of Eq.1 to 3 was carried out on data obtained over the period June 2008 to January 2015 and which will be considered as current data (Figures 3 and 4).

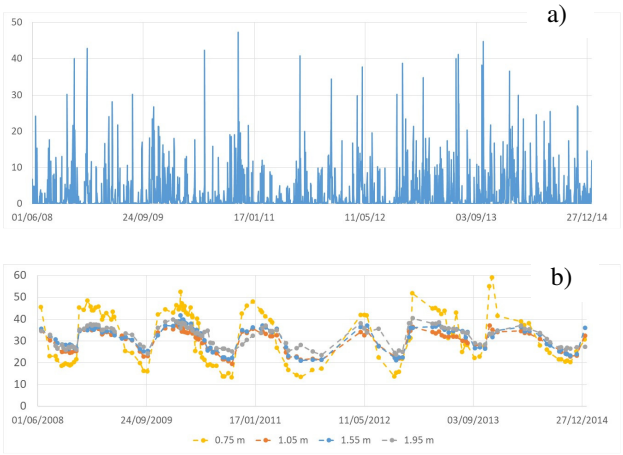

Figure 3: Daily precipitation (a) and volumetric water content (b) function of time at four depths (0.75m, 1.05m, 1.35m, 1.55m) in Bordeaux city.

Measurements of the volumetric water content θ were carried out over a depth of up to 3 m. They show that the measured θ at the site in question (medium-density urban area) varies between 20% and 95% throughout the year. Figure 4 shows, for illustrative purposes, the variability of the profile distribution of θ with depth for four different months.

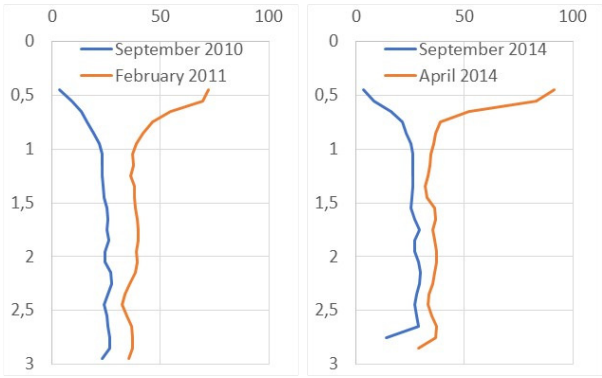

Figure 4: Profile distribution of θ with depth.

3. SOIL MOISTURE, SOIL-STRUCTURE INTERACTION AND MECHANICAL PIPE BEHAVIOR

The followed approach which is a probabilistic and reliability-based approach includes four main steps (Figure 5):

- The first step consists in defining a numerical model to transform the climate data (precipitation) in soil moisture as shown in § 2.

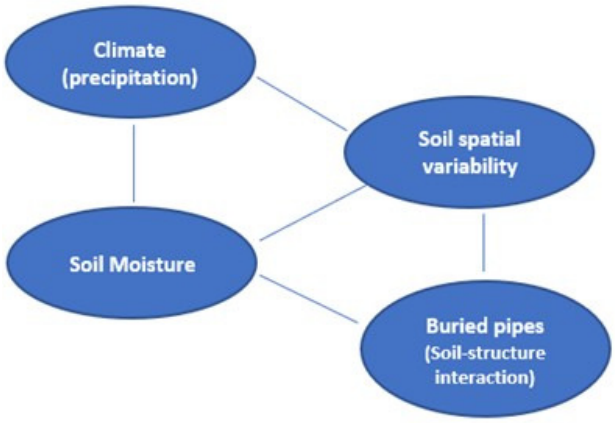

Figure 5: Schematic representation of the followed approach

- The second stage corresponds to the quantification of the sources of uncertainty which affect the studied problem (uncertainties relating to the loadings, soil spatial variability…). and identifying the

input parameters of the numerical model which are considered to be uncertain.

- The third step consists in building physical/numerical model which describes the behavior of a set of buried pipes and the soil-structure interaction.
- The last step corresponds to the propagation of the uncertainties affecting the input parameters through the numerical models and quantify the relative impact of the random variables at the input of the model on the hazard of the response.

3.1. Geo-mechanical behavior

The behavior of the set of pipes is driven by the soil-structure interaction between the rigid pipe (here in reinforced concrete) and the underlying soil. Each buried segmented pipe consists of a set of sections. Each section of finite length is decomposed into a number of beams connected to each other by nodes. At the ends of the sections, a pair of two independent nodes is used to represent the joints. Each pipe is subjected to earth load and surface load (by diffusion) and rests on a soil modeled, according to the Winkler model, by a set of independent springs with a coefficient of subgrade reaction k_s, in order to consider the soil-structure interaction (Elachachi et al., 2012). The effects of the two loads and their superposition depend on the burial depth. The pipe sections and the soil are considered to have a linear behavior.

3.2. Soil spatial variability

The variability and/or the uncertainty related to the volumetric water content θ and, consequently, to the coefficient of subgrade reaction k_s have three sources: the process of deposit and aggregation, the measurements uncertainties and the model uncertainty due for example to the relationship between the volumetric water content and the coefficient of subgrade reaction or in the expression of the soil-structure interaction itself.

However, the variability and uncertainties do not have the same consequences. Variability can create disorders when uncertainty only generates unawareness or ignorance. Since the role of the longitudinal variability of the soil appears essential, we chose to model it by using the theory of the local average of a random field developed by VanMarcke (1983).

The random field of the volumetric water content θ is defined by three properties: its average value θ_m, its variance σ_θ^2 and its scale of fluctuation S_f. This scale is related to a function of correlation $\rho(\Delta x)$ where Δx points out the distance between two points, and which describes the spatial structure of correlation of the soil properties. The exponential form has been chosen (Eq. 4):

$$\rho(\Delta x) = \exp\left(-2\frac{|\Delta x|}{S_f}\right) ;\ for\ \Delta x \leq S_f \qquad (4)$$

This scale of fluctuation S_f (length from which the correlation between soil properties tends to disappear) depends on the direction (horizontal or vertical).

3.3. Coefficient of subgrade reaction

There is no commonly accepted relationship in the literature directly relating soil stiffness or coefficient of soil reaction (a mechanical property) to volumetric water content θ (a physical property), this is a true epistemic uncertainty. Lu and Kaya (2014), based on experimental results, proposed the following power law equation (Eq. 5) between the soil modulus and θ:

$$E_s = E_d + (E_w - E_d)\left(\frac{\theta - \theta_d}{\theta_w - \theta_d}\right)^m \qquad (5)$$

where $E_s$is soil modulus; subscript d: dry state; w: wet state and m: empirical fitting parameter.

The transition to the coefficient of subgrade reaction is carried out through the Vesic equation (Elachachi, 2012):

$$k_s = \frac{0{,}65}{D}\sqrt[12]{\frac{E_s b^4}{E_c I}}\,\frac{E_s}{1-\nu_s^2} \qquad (6)$$

where ν_s is the Poisson ratio of the soil, D, I, E_c are respectively, diameter, moment of inertia and Young modulus of the concrete pipe.

3.4. Performance functions

The occurrence of failures in the buried pipes could affect the following three performances:

- Structural performance (SP): crack defects (hairline, radial or transverse) due to soil settlements.
- Hydraulic performance (HP): especially valid for stormwater or sewer pipes; differential settlements between the two ends of a pipe section induce a decrease of the network's effective flow due to siltation and counter-slopes. A too-high counter-slope harms the flow of effluents and may, for example, facilitate the clogging of the pipes via the sedimentation of suspended particles.
- Tightness performance (TP): segmented pipes are by definition not continuous. The presence of joints with weak stiffness, leads to joint openings, resulting in exfiltration and consequent harmful effects, such as environmental pollution in one way or the infiltration and possible erosion of the backfill in the opposite way.

The comparison between the effects of the various climate scenarios will be made on these three main performances and their corresponding indicators of performance I_{SP} , I_{HP} , and I_{TP} for the structural, hydraulic and tightness respectively.

These indicators are based on a reliability analysis (Lemaire 2013, Melchers and Beck, 2017) where limit state functions are expressed:

- By quantifying the cracking state (for a concrete pipe) in terms of bending stresses:

$$g_{SP} = \sigma_R - \sigma_S \quad (7)$$

where σ_R is the yield tension stress of concrete and σ_S is the maximum bending stress.

- In terms of counterslopes. The corresponding limit state function is as follows:

$$g_{HP} = CS_R - CS_S \quad (8)$$

where CS_R is the maximum acceptable counterslope and CS_S is the maximum computed counterslope.

- In terms of a joint opening with a limit state function:

$$g_{TP} = OJ_R - OJ_S \quad (9)$$

where OJ_R is the maximum acceptable joint opening and OJ_S is the maximum computed joint opening.

Insofar as no consensus exists in the literature on the choice of the probability distribution function a Lognormal distribution is chosen for almost all aleatory soil and pipe parameters.

The Hasofer–Lind reliability index β is defined by the following equation (Eq. 10):

$$\beta = \frac{ln\left\{\frac{R}{S}[(1+CoV_S^2)/(1+CoV_R^2)]^{1/2}\right\}}{\{ln[(1+CoV_S^2)(1+CoV_R^2)]\}^{1/2}} \quad (10)$$

where subscript R, S mean, respectively, resistance and mean maximum demand (stress, counterslope or joint opening) with their respective coefficients of variation CoV. The corresponding individual probability of failure is $P_{fg} = \Phi(-\beta)$. Finally, the indicators of performance are defined for the three performances as:

$$I_i = \frac{\beta_{ref\_i}}{\beta_{case\_i}} \;\; ; \;\; i = SP, HP \; or \; TP \quad (11)$$

where β_{case_i} is the reliability index corresponding to the analyzed climate scenario and β_{ref_i} is the reliability index corresponding to the current climate.

The obtained indicators of performance must be considered comparatively, rather than in an absolute manner, due to the following reasons:

- The arbitrary character of the values taken for the acceptable values of "resistance".
- The probability distribution function.
- The model uncertainties.

The higher these indicators, the worse the situation under study is.

4. STUDY CASES

In order to analyze the effects of climate change some cases are studied hereafter.

The reference case corresponds to the current climate (period from 2008 to 2020). All the performance indicators will be computed against this reference case.

The time horizons defined in the three climate scenarios, are studied hereafter: 2021-2050, 2041-2070 and 2070-2100. The combination with the three climate scenarios RCP2.6, RCP4.5 and RCP8.5 constitutes nine case studies shown in Table 1.

Table 1: Climate cases for several time horizons.

RCP	*Time horizons*		
	2021-50	*2041-70*	*2071-100*
RCP2.6	*Case 2-A*	*Case 2-B*	*Case 2-C*
RCP4.5	*Case 4-A*	*Case 4-B*	*Case 4-C*
RCP8.5	*Case 8-A*	*Case 8-B*	*Case 8-C*

The physical case study investigated in this paper is a section of pipes located in a semi-urbanized housing estate impervious at a level of 60%. The rainfall and the current soil water content were presented in Figures 3 and 4. The pipe crosses a soil composed mainly of silty to clay-silty sands for half and clays for the other half.

The geometric parameters of the pipe section are given in Table 2. The section length (90 m) corresponds to the classic distance between two manholes in France. It is made of 30 individual pipe segments. The joints are considered as semi-rigid. The resistance values which could be assumed for reinforced concrete pipes belonging to stormwater or sewer networks are presented in Table 3.

Table 2: Pipe parameters.

Diameter	*1 m*	*Length*	*90 m*
Thickness	*0.1m*	*Joint stiff.*	*0,4 MN/m*
E_c	*30 GPa*	*Material*	*R.C.*

Table 3: Statistical values of resistance variables.

Variable	*mean*	*Standard deviation*
σ_R	*3.0 MPa*	*0.45 MPa*
CS_R	*5%*	*1.5%*
OJ_R	*2°*	*0.5°*

The soil parameters (for Eq.4 and 5) are as for them given in Table 4. Its scale of fluctuation S_f is taken equal to 10 m. The effect of this parameter is very important but is not presented here (see Elachachi and al., 2012)

Table 4: Soil parameters.

ν_s	*0.3*	θ_r	*0.20*
Layer depth	*5 m*	θ_w	*0.95*
S_f	*10 m*	*Coeff.m*	*0.4*

The numerical computations are carried out according to the Monte Carlo process (LHS sampling, Lemaire 2013). All the results detailed below have been obtained from the data processing of outputs in a series of 10^5 simulations.

4.1. Climate scenario and intermediate results

Figure 6 shows cumulative distribution functions of outputs for structural, hydraulic and tightness performance, namely bending stresses (a), counterslopes (b) and opening joints (c) for the current case compared to seasonal results for the case 4-A of Table 1.

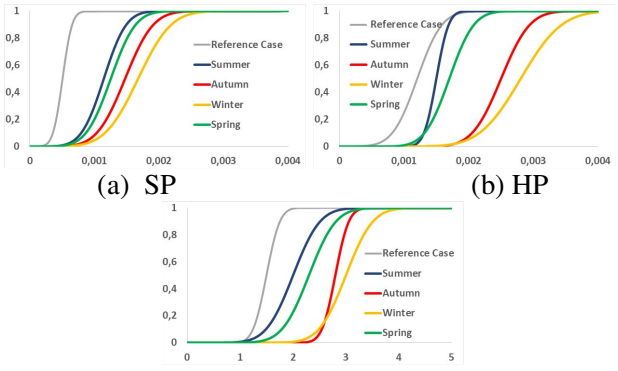

(a) SP (b) HP

(c) TP

Figure 6: Comparison of cdf between current case and case 4-A.

It is shown that the autumn/winter outputs are more pronounced than those of the spring/summer seasons on the one hand and that the dispersion is not identical for all the seasons on the other hand. For example, the mean counterslope value in the winter according to the RCP4.5 during 2021-2050 period is 2.33 times larger than the reference

(current) case while the dispersion is 1.7 times larger (Figure 6.b). Whereas if we are interested in opening joints, we find ratios for the same cases of 3.31 and 3.45 respectively (Figure 6.c). From these first outputs, we are able to estimate the reliability index (Eq. 10) of each situation, then to quantify the different indicators corresponding to each performance and each season (Eq. 11). Figure 7 illustrates this kind of results for the same case 4-A. The level of the reliability is different depending on the considered performance and the season (Figure 7.a).

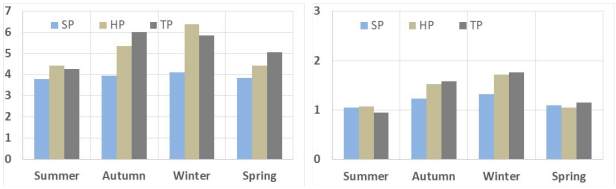

(a) (b)

Figure 7: Reliability indices (a) and Performance indicators (b) for the case 4-A.

Consequently, the indicators of performance (Figure 7.b) are comprised between 0.95 and 1.77. To remind, an index close to 1 indicates that we observe the same failure rates as the current period. Then, the higher they are, the higher the failure rate as well.

4.2. Comparing of Performance functions and climate scenarios

The proposed approach is generalized to the different scenarios identified in §1. The analysis that must be made, given the level of uncertainty assumed in these scenarios, will be relative and not absolute.

Figures 8 to 10 show clearly the effects of climate change on buried pipe behavior and potential failure rates. For structural performance, the indicator and therefore the failure rate can be up to 3 times the currently estimated rate if the worst-case scenario, scenario RCP8.5 takes place.

This failure rate can go up to almost 7 times the current one for the performance related to the tightness of the pipe system. The seasonal variations are quite similar for all scenarios, with the autumn and winter periods seeming to be the most unfavorable.

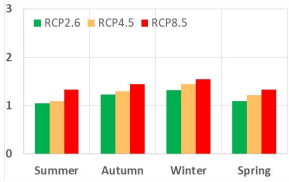

I_{SP}: Cases 2-A, 4-A, 8-A

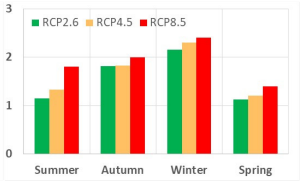

I_{SP}: Cases 2-B, 4-B, 8-B

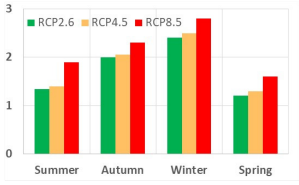

I_{SP}: Cases 2-C, 4-C, 8-C

Figure 8: Structural Indicator of performance I_{SP}.

This observation should be put into perspective with the type of soil selected for this study. If the soil was of the swelling clay type, one can suppose that dry periods may be more harmful than wet periods.

5. CONCLUSIONS

A methodology is developed and presented in this study in order to assess the effect of climate change on the behavior of segmented buried pipes and in particular pipes belonging to sewerage or stormwater networks that operate by gravity flow. Two simple models were developed. The first one allows to transform weather data (precipitation), in soil moisture knowing the characteristics of the soil (permeability, degree of soil sealing…).

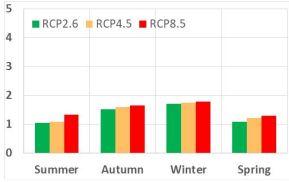

I_{HP}: Cases 2-A, 4-A, 8-A

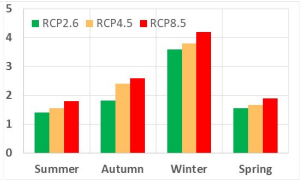

I_{HP}: Cases 2-B, 4-B, 8-B

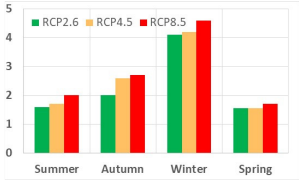

I_{HP}: Cases 2-C, 4-C, 8-C

Figure 9: Hydraulic Indicator of performance I_{HP}.

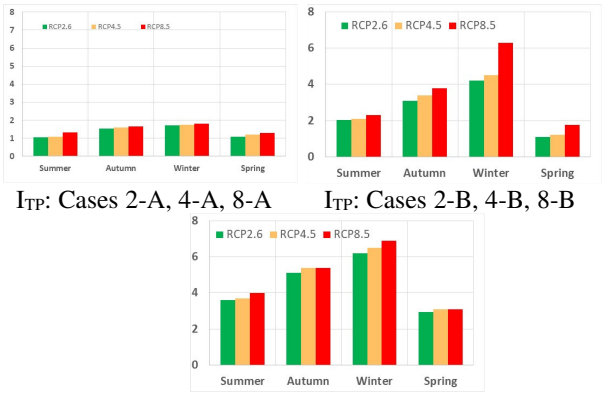

I_{TP}: Cases 2-A, 4-A, 8-A I_{TP}: Cases 2-B, 4-B, 8-B

I_{TP}: Cases 2-C, 4-C, 8-C

Figure 10: Tightness Indicator of performance I_{TP}.

The second one includes the soil-pipe interaction and considers the spatio-temporal variability of the soil moisture in a geo-mechanical numerical model. All this within a probabilistic and reliability-based framework.

In combination with climate scenario predictions, the variation in three kinds of indicators of performance as a result of climate change is estimated. Several uncertainties in the extrapolation of results are considered.

This holistic view of failure consequences could be included for counting direct and indirect damages in a risk-based framework.

6. REFERENCES

Breysse, D., C. La Borderie, S. M. Elachachi, and H. Niandou. (2007). "Spatial variations in soil properties and their influence on structural reliability." *Civil Engineering and Environmental Systems*, 24(2): 73–83.

DRIAS, (2021). "The new reference climate projections for France", DRIAS Project, (Donner accès aux scénarios climatiques Régionalisés français pour l'Impact et l'Adaptation de nos Sociétés et environnement, (in French).

Elachachi S.M., Breysse D., Denis A. (2012). The effects of soil spatial variability on the reliability of rigid buried pipes. *Computers and Geotechnics*, 43, 61–71.

Entekhabi, D., Rodriguez-Iturbe, I., and Castelli, F. (1996). "Mutual Interaction of Soil Moisture State and Atmospheric Processes". *Journal of Hydrology*, 184, 3-17.

Lemaire M., 2013., "Structural reliability", *Wiley-ISTE*.

Lu, N., and Kaya, M. (2014). "Power law for elastic moduli of unsaturated soil." *ASCE J. Geotech. Geoenviron. Eng.*, 140(1), 46-56.

Melchers R.E., Beck A.T., (2017). "Structural Reliability Analysis and Prediction", *John Wiley & Sons Ltd.*

Rodriguez-Iturbe I., Porporato A., (2004). "Ecohydrology of Water Controlled Ecosystems ", Cambridge University Press.

Shepherd, T. (2014), "Atmospheric circulation as a source of uncertainty in climate change projections", *Nature Geoscience*, 7(10), pp. 703-708.

Singh N.K., Emanuel R.E., McGlynn B.L., Miniat C.F., (2021). "Soil Moisture Responses to Rainfall: Implications for Runoff Generation", *Water Resources Research*, 57(9).

Wols, B.A., Van Thienen, P. 2014, "Modelling the effect of climate change induced soil settling on drinking water distribution pipes", *Computers and Geotechnics* 55, 240–247.

Wuebbles, D.J., D.R. Easterling, K. Hayhoe, T. Knutson, R.E. Kopp, J.P. Kossin, K.E. Kunkel, A.N. LeGrande, C. Mears, W.V. Sweet, P.C. Taylor, R.S. Vose, and M.F. Wehner, (2017): "Our globally changing climate". In *Climate Science Special Report: 4th National Climate Assessment*, Vol.I., U.S. Global Change Research Program, pp. 35-72.

VanMarcke, E.H, 1983, "Random Fields: Analysis & Synthesis", *MIT Press, Cambridge*, 383p.